C. R. Geoscience 334 (2002) 303–311

S1631-0713(02)01760-1/FLA

Géomatériaux / Geomaterials
(Minéralogie / Mineralogy)

Discovery of an alkaline orthogneiss in the eclogite-bearing Cellier Unit (Champtoceaux Complex, Armorican Massif): a new witness of the Ordovician rifting

Michel Ballèvre[a,*], Ramon Capdevila[a], Catherine Guerrot[b], Jean-Jacques Peucat[a]

[a] *Géosciences Rennes, UMR 6118, université Rennes-1, 35042 Rennes cedex, France*
[b] *BRGM, service « Analyse et caractérisation minérale », BP 6009, 45060 Orléans cedex 2, France*

Received 17 September 2001; accepted 7 January 2002

Communicated by Jean Dercourt

Abstract – An alkaline orthogneiss from the Lower Allochton of the Champtoceaux Complex has been identified by its mineralogy and its whole-rock chemistry, including trace elements and Sr and Nd isotopes. An U/Pb study of the zircons using the conventional method gives an upper intercept age of 481 +6/−5 Ma. The alkaline orthogneiss is thus a new witness of the Ordovician rifting in the Variscan Belt. ***To cite this article: M. Ballèvre et al., C. R. Geoscience 334 (2002) 303–311.*** © 2002 Académie des sciences / Éditions scientifiques et médicales Elsevier SAS

alkaline orthogneiss / Ordovician / Variscan Belt / Champtoceaux Complex / Armorican massif / France

Résumé – Découverte d'un orthogneiss alcalin dans l'unité du Cellier (complexe de Champtoceaux, Massif armoricain) : un nouveau témoin du *rifting* ordovicien. Dans l'allochtone inférieur du complexe de Champtoceaux (Massif armoricain) a été découvert pour la première fois un orthogneiss dont les caractéristiques minéralogiques et la composition chimique (majeurs, traces et isotopes du Sr et du Nd) montrent qu'il dérive d'un magma alcalin. Une étude U–Pb sur zircons par la méthode conventionnelle a fourni un âge par intercept supérieur de 481 +6/−5 Ma, qui est interprété comme l'âge de cristallisation du protolithe. L'orthogneiss alcalin est donc un nouveau témoin du *rifting* ordovicien. ***Pour citer cet article : M. Ballèvre et al., C. R. Geoscience 334 (2002) 303–311.*** © 2002 Académie des sciences / Éditions scientifiques et médicales Elsevier SAS

orthogneiss alcalin / Ordovicien / Chaîne varisque / complexe de Champtoceaux / Massif armoricain / France

Version abrégée

1. Introduction

La Chaîne hercynienne comprend de nombreux témoins d'un magmatisme cambro-ordovicien. Leur étude géochimique révèle l'existence de magmas calco-alcalins, indiquant l'existence d'une zone de subduction active à cette époque [5], ou/et de magmas alcalins, parfois même hyperalcalins, suggérant, au contraire, l'existence d'un épisode de distension intracontinentale [8, 32]. Savoir si ces deux types de magmas ont coexisté ou se sont succédé dans le temps et/ou dans l'espace est une question essentielle, qui requiert une analyse détaillée des orthogneiss. Dans ce cadre, cette note signale l'existence d'un orthogneiss alcalin, d'âge Ordovicien inférieur, dans le complexe de Champtoceaux.

2. Contexte géologique

Dans le Massif armoricain, de nombreux orthogneiss cambro-ordoviciens ont été identifiés [17]. Tel est en particulier le cas dans le complexe de Champtoceaux [1, 7, 24], un empilement d'écailles ultérieurement plissé en une vaste

* Correspondence and reprints.
E-mail address: Michel.Ballevre@univ-rennes1.fr (M. Ballèvre).

antiforme d'axe est–ouest (Fig. 1). Le parautochtone présente des *metagrauwackes* d'âge inconnu. Tant l'allochtone inférieur que l'allochtone moyen comprennent de grandes quantités d'orthogneiss leucocrates à grain fin (leptynites). Certains orthogneiss dérivent de granites, comme le montrent non seulement de rares volumes non déformés [20], mais aussi la présence de reliques de cornéennes, témoins du métamorphisme de contact de ces granites [25]. La présence d'un litage décimétrique à décamétrique dans la plupart des orthogneiss suggère cependant une dérivation à partir de volcanites ou d'intrusions hypovolcaniques. Dans l'allochtone inférieur (Fig. 1), les leptynites contiennent de nombreuses lentilles éclogitiques, qui dérivent de filons ou de sills doléritiques [13].

Jusqu'à présent, deux orthogneiss ont été datés dans l'allochtone inférieur du complexe de Champtoceaux. Le premier est un métagranite coronitique (la Picherais), pour lequel un âge Silurien (U/Pb sur zircons, intercept bas à 423 ± 10 Ma) a été proposé [38]. Le second est un orthogneiss leucocrate (orthogneiss de Saint-Mars-du-Désert), qui a été daté de l'Ordovicien inférieur (U/Pb sur zircons, intercept haut à 485 ± 11 Ma) [28]. L'affinité magmatique de ces deux orthogneiss n'a cependant pas été établie, de sorte que leur signification reste conjecturale.

3. Pétrographie et minéralogie

L'orthogneiss étudié a été récolté au Cellier, sur la rive droite de la Loire (Fig. 1), au bord de la voie de chemin de fer. L'unité du Cellier, qui affleure là dans de bonnes conditions, est essentiellement constituée de leptynites, avec de nombreuses lentilles d'éclogites. Les leptynites sont représentées par des faciès fins, avec parfois des niveaux d'épaisseur métrique de gneiss œillés (avec des porphyroclastes de feldspath potassique ayant jusqu'à 5 cm de longueur), intensément déformés. La plupart des orthogneiss (par exemple, CEL 22) contiennent, outre quartz et feldspaths, épidote, muscovite et grenat. Dans un niveau (CEL 23) ont été observés quartz, albite et feldspath potassique, ainsi que des quantités mineures d'une biotite fortement pléochroïque (environ 3%) et d'une amphibole bleu–vert (environ 2%). Les analyses à la microsonde électronique (Tableau 1) montrent que la biotite, pauvre en TiO_2, est ferrifère (Fig. 2). Quant à l'amphibole, il s'agit également d'une espèce ferrifère, en l'occurrence une hastingsite dans la classification internationale (Tableau 1). Un grenat calcique ($X_{Grs} = 0{,}36$) est seulement rarement observé. Sphène, zircon, apatite, allanite, magnétite et pyrite sont également présents.

4. Géochimie

L'analyse chimique de l'échantillon CEL 23 (Tableau 2) montre que la roche étudiée est une roche magmatique n'ayant pas été significativement altérée, sauf peut-être pour le Cs. La roche est riche en Si, relativement pauvre en Al et Fe, et pauvre à très pauvre en Ti, Ca, Mg et P. L'échantillon est relativement riche en alcalins, avec un rapport K_2O/Na_2O voisin de 1,1. Ces caractéristiques sont celles d'un granite à feldspaths alcalins, riche en potassium, faiblement saturé en alumine (A/CNK ca 1) et ferrifère ($Mg/(Fe + Mg) < 0{,}1$). Dans le détail, les éléments en traces montrent que le protolithe de l'échantillon CEL 23 était un granite (ou une rhyolite) de type A1 [10, 11].

Le rapport ε_{Nd} à 480 Ma est d'environ +1 (Tableau 3), en accord avec les valeurs mesurées pour des roches similaires en Galice, dans le Nord-Ouest de l'Espagne [33]. Le magma alcalin pourrait être issu d'un manteau appauvri, avec éventuellement une faible composante crustale à partir d'une source à 2 Ga, telle qu'elle est connue dans le Nord du Massif armoricain [14]. Le rapport initial du Sr à 480 Ma (0,702) est compatible avec le composant mantellique défini ci-dessus, mais peut également résulter d'une perturbation du système Rb/Sr durant le métamorphisme.

5. Géochronologie

Une étude U–Pb sur zircons de l'échantillon CEL 23 a été effectuée par la méthode conventionnelle (Tableau 4). Les zircons, nombreux, appartiennent aux types S22, P3 ou P5 dans la classification de Pupin [34], types qui sont généralement observés dans les magmas calco-alcalins ou alcalins de haute température. Les zircons ont été séparés et abrasés [18, 19, 26], leur analyse étant réalisée sur un spectromètre Finnigan Mat 261. Les six fractions s'alignent sur une discordia, dont l'intercept supérieur, à 481 ± 6 Ma (Fig. 4), est interprété comme l'âge de cristallisation du protolithe magmatique de l'orthogneiss alcalin.

6. Conclusion

Les gneiss à biotite-hastingsite de l'unité du Cellier (allochtone inférieur du complexe de Champtoceaux) dérivent d'intrusions superficielles (ou éventuellement de volcanites) alcalines, ayant cristallisé aux environs de 480 Ma (Ordovicien inférieur). Il s'agit donc d'un nouveau témoin du magmatisme alcalin, antérieurement identifié dans le Massif armoricain en Choletais [22, 36] et dans la région de Concarneau [15, 37]. Ce magmatisme est le témoin du *rifting* ordovicien qui affecte largement tout le domaine occupé ultérieurement par la Chaîne hercynienne.

1. Introduction

Identifying the nature and age of the pre-orogenic magmatism in the Variscan Belt is a prime tool for unraveling its plate tectonic development before the final collision during the Carboniferous. The Cambro-Ordovician age of a large part of the pre-orogenic magmatism has been recognised during the past years.

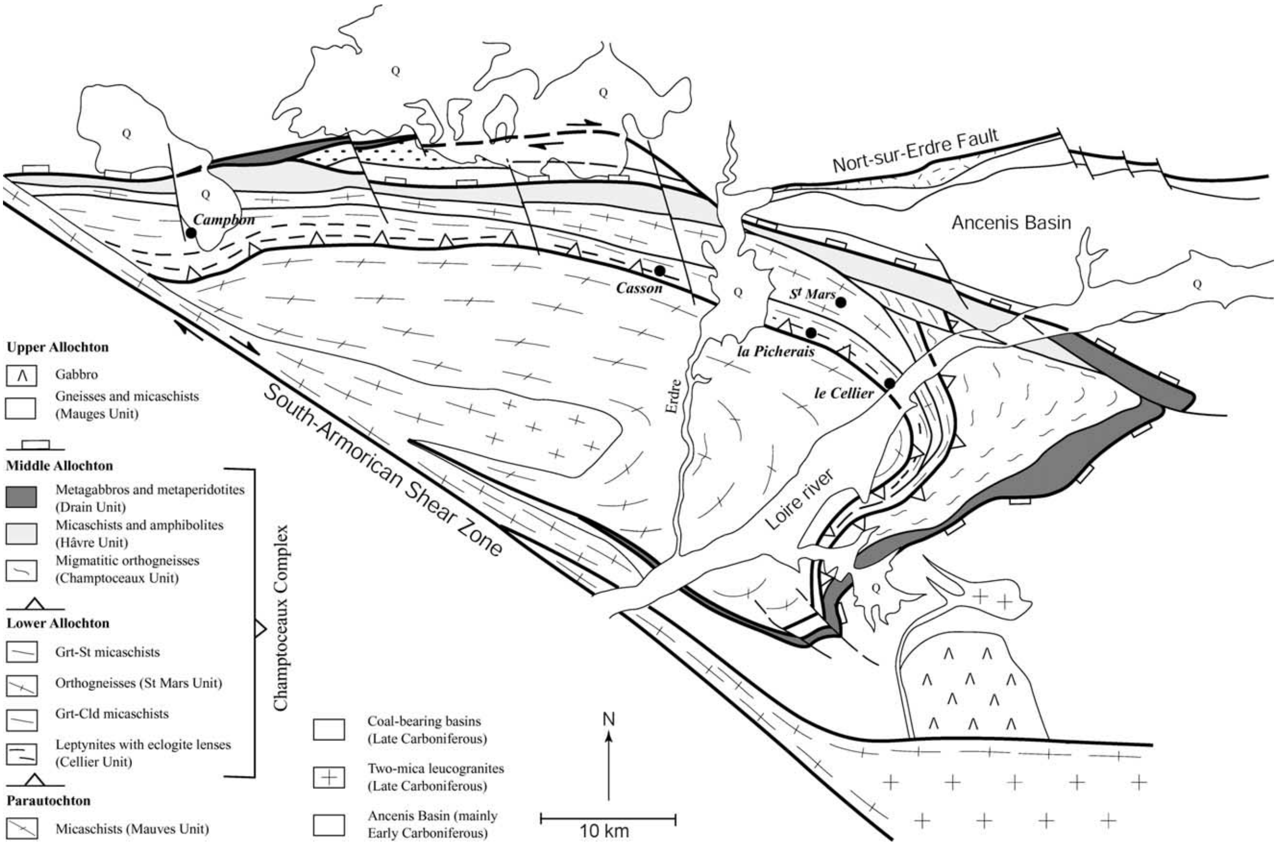

Figure 1. Simplified geological map of the Champtoceaux Complex (modified after [3]). The studied orthogneiss has been sampled at le Cellier, along the right bank of the Loire River.

Figure 1. Carte du complexe de Champtoceaux (modifiée d'après [3]). L'orthogneiss étudié a été échantillonné au Cellier, sur la rive droite de la Loire.

The geochemistry of the Cambro-Ordovician felsic magmatism presents either calc-alkaline affinity, indicative of subduction processes (e.g., [5]), or alkaline (and even peralkaline) affinities, suggesting continental rifting (e.g., [8, 32]). Whether the two types of magmas occur synchronously in different parts of the Variscan Belt or diachronously in the same unit requires detailed knowledge of their age.

In the Armorican Massif, pre-orogenic orthogneisses are found in a large area, including the Leon in its northwestern part, a few bodies in its northern and central parts, as well as numerous bodies in the South-Armorican Domain. The petrology of most of these bodies is poorly known. This paper represents a contribution towards a better understanding of the felsic orthogneisses from the Champtoceaux Complex. Previous work in this Complex led to the recognition of (*i*) a poorly defined Silurian age (423 ± 10 Ma) for a coronitic metagranite [38], and (*ii*) Early Ordovician (485 ± 11 Ma) protoliths for the Saint-Mars-du-Désert orthogneiss [28]. The magmatic affinity of both bodies has not been investigated.

2. Geological setting

The Champtoceaux Complex [1, 7, 24] consists of several stacked units, later refolded by a large-scale, east–west trending antiform (Fig. 1). The Parautochton displays monotonous metagreywackes of unknown age. Both the Lower Allochton and the Middle Allochton contain large amounts of fine-grained, leucocratic, orthogneisses. In the Lower Allochton, the Cellier Unit is characterised by orthogneisses displaying numerous, well-preserved, eclogite lenses.

Evidence for the nature of the orthogneisses of the Cellier Unit before the ductile deformation is rarely preserved. Metre-scale undeformed pods with a well-preserved granitic texture occur at la Picherais (Fig. 1) within strongly sheared gneisses [20]. Most outcrops or quarries show strongly deformed gneisses that present a faint to well-defined layering at decimetre to decametre scale. In particular, layers of augen-gneisses (with up to 5 cm long K-feldspar porphyroclasts) up to a few metres in thickness are present. Dark microgranular enclaves have been recognised in the undeformed pod at la Picherais, but are not found

Table 1. Representative chemical analyses (Microsonde Ouest, Brest) of some minerals from sample CEL 23.

Tableau 1. Compositions chimiques représentatives (Microsonde Ouest, Brest) de quelques minéraux de l'échantillon CEL 23.

	CEL 23									CEL 23A									
	Pl clast 7	Pl matrix 21	Kfs matrix 23	Bt inclusion 11	Bt matrix 26	Amp matrix 19	Amp matrix 53	Ttn matrix 35	Apatite matrix 65	Pl clast 15	Pl matrix 26	Kfs inclusion 19	Kfs matrix 25	Bt matrix 22	Bt matrix 24	Grt core 3	Grt rim 2	Rt inclusion 45	Ttn matrix 46
SiO_2	69.05	69.04	65.23	34.55	34.96	37.63	37.76	30.50	0.15	69.08	68.24	64.67	64.15	33.56	33.99	36.79	37.11	0.51	31.21
TiO_2	0.07	0.00	0.00	0.80	2.34	0.31	0.30	28.38	0.00	0.00	0.00	0.01	0.00	2.41	2.99	0.12	0.05	92.60	27.60
Al_2O_3	19.05	19.55	17.75	16.78	13.86	11.53	11.37	5.75	0.00	19.56	19.83	18.26	18.33	13.92	14.62	20.76	19.64	0.56	7.38
Cr_2O_3	0.08	0.00	0.03	0.00	0.00	0.00	0.03	0.00	0.00	0.01	0.02	0.00	0.00	0.00	0.09	0.01	0.00	0.00	0.00
$Fe_2O_3^*$								2.69											1.30
FeO^*	0.16	0.00	0.08	33.00	34.96	33.03	31.46		0.05	0.02	0.06	0.08	0.02	33.57	33.05	21.99	24.11	1.38	
MnO	0.00	0.12	0.05	0.48	0.43	0.85	0.74	0.16	0.02	0.00	0.06	0.07	0.02	0.10	0.37	6.43	3.28	0.00	0.08
MgO	0.00	0.00	0.00	0.56	0.66	0.33	1.79	0.00	0.00	0.00	0.00	0.00	0.00	1.47	0.78	0.01	0.02	0.01	0.00
CaO	0.04	0.20	0.00	0.00	0.00	9.89	10.95	27.88	57.06	0.07	0.39	0.01	0.00	0.01	0.02	13.02	14.77	0.31	27.70
Na_2O	12.14	11.81	0.21	0.05	0.05	1.81	1.72	0.02	0.07	11.81	11.71	0.31	0.32	0.06	0.04	0.16	0.03	0.03	0.18
K_2O	0.09	0.12	17.54	9.61	9.57	2.66	2.42	0.00	0.01	0.23	0.11	17.25	17.41	9.61	9.25	0.00	0.02	0.04	0.00
P_2O_5									43.24										
	100.68	100.84	100.89	95.83	96.83	98.04	98.54	95.38	100.60	100.78	100.42	100.66	100.25	94.71	95.20	99.29	99.03	95.44	95.45
O	8	8	8	22	22	23	23		12	8	8	8	8	22	22	24	24	2	
Si	3.003	2.994	3.010	5.631	5.710	6.157	6.092	1.009	0.012	2.996	2.975	2.989	2.981	5.597	5.601	5.917	5.987	0.007	1.021
Ti	0.002	0.000	0.000	0.098	0.288	0.038	0.036	0.706	0.000	0.000	0.000	0.000	0.000	0.302	0.371	0.015	0.006	0.975	0.679
Al	0.976	0.999	0.965	3.221	2.666	2.224	2.162	0.224	0.000	1.000	1.019	0.995	1.004	2.734	2.837	3.937	3.735	0.009	0.284
Cr	0.003	0.000	0.001	0.000	0.000	0.000	0.004	0.000	0.000	0.000	0.001	0.000	0.000	0.000	0.012	0.001	0.000	0.000	0.000
Fe^{3+}						0.438	0.514	0.067											0.032
Fe^{2+}	0.006	0.000	0.003	4.498	4.776	4.120	3.775		0.003	0.001	0.002	0.003	0.001	4.682	4.554	2.958	3.253	0.016	
Mn	0.000	0.004	0.002	0.066	0.059	0.118	0.101	0.004	0.001	0.000	0.002	0.003	0.001	0.014	0.052	0.876	0.448	0.000	0.002
Mg	0.000	0.000	0.000	0.136	0.161	0.081	0.435	0.000	0.000	0.000	0.000	0.000	0.000	0.365	0.192	0.002	0.005	0.000	0.000
Ca	0.002	0.009	0.000	0.000	0.000	1.734	1.893	0.988	4.792	0.003	0.018	0.000	0.000	0.002	0.004	2.244	2.553	0.005	0.971
Na	1.023	0.993	0.019	0.016	0.016	0.574	0.538	0.001	0.011	0.993	0.990	0.028	0.029	0.019	0.013	0.050	0.009	0.001	0.011
K	0.005	0.007	1.032	1.998	1.994	0.555	0.498	0.000	0.001	0.013	0.006	1.017	1.032	2.045	1.944	0.000	0.004	0.001	0.000
P									2.870										
	5.020	5.006	5.032	15.664	15.670	16.039	16.048	2.999	7.690	5.006	5.013	5.035	5.048	15.760	15.580	16.000	16.000	1.014	3.000
															Alm	46.46	49.61		
															Sps	15.02	7.51		
															Prp	0.04	0.08		
															Grs	32.39	35.49		
															And	6.05	7.30		

in the deformed gneisses. Other evidence in favour of the intrusive character of part of the protoliths of the gneisses is the discovery of relics of hornfelses, at Casson and Campbon (Fig. 1) [25]. Nevertheless, the lack of homogeneity and the obvious layering argues in favour of volcanic or high-level intrusions rather than huge plutons.

The eclogite lenses from the Cellier Unit most probably derive from doleritic sills or dykes, as recorded by peculiar texture in undeformed samples [13]. This is consistent with their restricted bulk-rock chemistry, basaltic whole-rock compositions similar to N-MORBs to P-MORBs [27]. During high-pressure metamorphism, the metadolerites have been converted into a fine-grained assemblage of garnet–omphacite–amphibole–rutile [13].

The age relationships between the eclogites and the surrounding gneisses cannot be determined accurately on the field. Relics of high-pressure parageneses are rarely found in the orthogneisses, where they consist of high-Si phengite and grossular-rich garnet [3, 21]. In addition, the garnet corona around biotite in the undeformed pod at la Picherais, once thought to develop during a granulite-facies event [20], is now regarded as a witness of an incomplete reequilibration during the eclogite-facies event.

3. Petrography and mineralogy

The leucocratic gneisses from the Cellier Unit can be divided into two broad categories. Most gneisses are "calc-alkaline" gneisses, containing epidote, garnet, biotite and muscovite as key phases (CEL 22). Rare examples of "alkaline" gneisses contain a strongly pleochroic biotite and a blue-green amphibole. The studied samples (CEL 23 and CEL 23A) have been collected along the right bank of the Loire River, close to the village of le Cellier, where the railway section provides a nice exposure of the Champtoceaux Complex. The studied samples are fine-grained leucocratic gneisses, displaying a well-developed foliation. Microscopic examination reveals that quartz and feldspar are modally dominant phases (33% Qtz, 37% Pl and 24.5% Kfs) and that foliation is defined by minute grains of biotite (3%) and amphibole (2%).

Two types of plagioclase grains are found, with larger, weakly strained, grains displaying albite twins that are surrounded by a fine- to very-fine grained matrix consisting of minute plagioclase, microcline and quartz grains. Ferromagnesian minerals include abundant biotite lamellae with a very strong pleochroism (from pale yellow–brown to dark brown), prismatic amphibole crystals with a strong pleochroism (from pale yellow–green to blue–green to green), and very rare garnet ($< 0.5\%$) and clinozoisite (ca 0.1%). Minor variations in modal proportions show that biotite

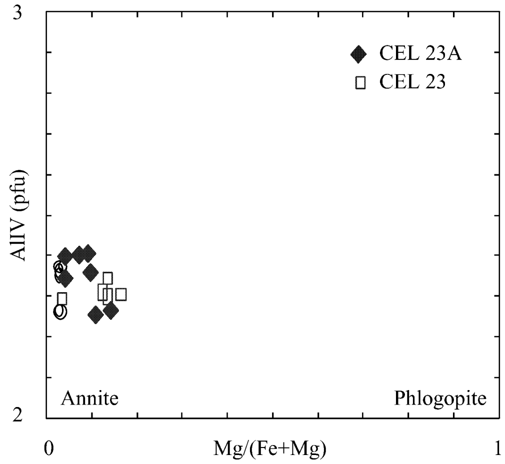

Figure 2. Mineral chemistry of biotite from the Cellier orthogneiss.

Figure 2. Composition chimique de la biotite de l'orthogneiss du Cellier.

and amphibole coexist in some layers, whereas biotite $\pm$ garnet is stable in other layers. Titanite (ca 0.3%), zircon, apatite, allanite, magnetite and pyrite are also present.

Microprobe analyses have been performed with the Microsonde Ouest (Brest) using the following analytical conditions: 15 kV acceleration voltage, 20 nA sample current, 10 s counting time. Representative mineral compositions are given in Table 1. *Plagioclase* grains are close to albite end-member, whether they are large blasts (with no core to rim variation) or fine-grained matrix. The *K-feldspar* composition is also close to end-member. *Biotite* grains are Al-poor and Fe-rich, thus plotting close to the annite end-member (Fig. 2). In addition, their TiO_2 content is relatively low. *Amphibole* grains are calcic varieties, which plot in the IMA classification in the hastingsite field, close to the hastingsitic hornblende field. *Garnet* is an almandine–grossular–spessartine solid solution, with minor core-to-rim zonation (decreasing spessartine and increasing almandine and grossular). The high grossular content (up to 36 mol per cent) is a characteristic feature of the garnets from the orthogneisses of the Cellier Unit [21]. *Rutile* is rarely observed (sample CEL 23A), and is rimmed by *titanite*, the latter being also present in the matrix. Titanite shows a relatively high $Al + Fe^{3+}$ content (up to 0.34 pfu), with $Al \gg Fe^{3+}$.

4. Geochemistry

The chemical composition of sample CEL 23 (Table 2) is that of a magmatic rock that has not been altered significantly, except perhaps for Cs. The rock is rich in Si, relatively poor in Al and Fe, and poor to very poor in Ti, Ca, Mg and P. The sample is relatively rich in alkali, with a K_2O/Na_2O ratio

Table 2. Whole-rock chemistry of sample CEL 23 (CRPG, Nancy). Major elements (in weight %) were analysed by ICP–AES, trace elements (in ppm) by ICP–MS.

Tableau 2. Composition chimique de l'échantillon CEL 23 (CRPG, Nancy). Les éléments majeurs (en pourcentages pondéraux) ont été analysés par ICP–AES, les éléments en traces (en ppm) par ICP–MS.

SiO_2	TiO_2	Al_2O_3	Fe_2O_3	MnO	MgO	CaO	Na_2O	K_2O	P_2O_5	LOI	Total
75.66	0.13	12.23	1.68	< 0.03	0.09	0.36	4.07	4.44	0.03	1.04	99.73
Cs	**Rb**	**Ba**	**W**	**Th**	**U**	**Ta**	**Nb**	**Pb**	**Sr**	**Zr**	**Hf**
0.911	109.7	181	0.75	17.85	4.29	3.88	48.89	9.8	34.3	304	9.06
Sn	**Be**	**Y**	**Ga**	**V**	**Co**	**Zn**	**Cu**	**Cr**	**Ni**	**La**	**Ce**
2.81	2.3	41.3	24.8	2.47	0.56	38	5.1	13.3	2.34	64.06	130.3
Pr	**Nd**	**Sm**	**Eu**	**Gd**	**Tb**	**Dy**	**Ho**	**Er**	**Tm**	**Yb**	**Lu**
14.58	52.74	10.42	0.447	8.53	1.27	7.97	1.56	4.27	0.67	4.55	0.61

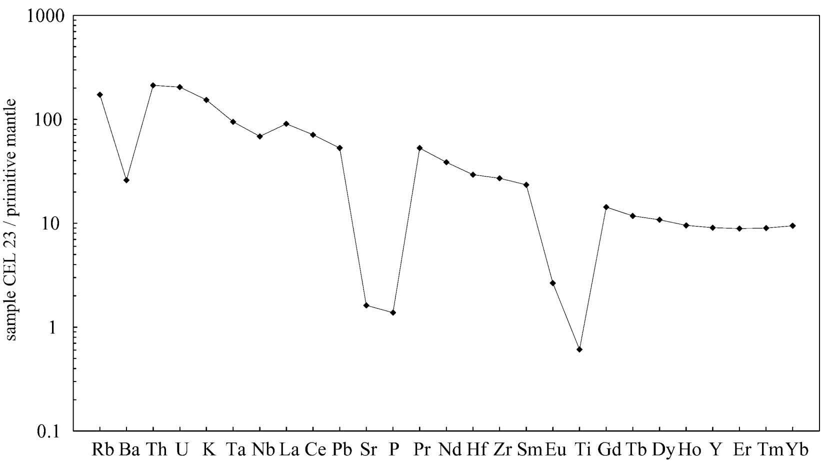

Figure 3. Diagram normalised to the primitive mantle of sample CEL 23.

Figure 3. Diagramme normalisé au manteau primitif de l'échantillon CEL 23.

Table 3. Sm/Nd and Rb/Sr isotopic data for sample CEL 23 (Géosciences Rennes).

Tableau 3. Données isotopiques Sm/Nd et Rb/Sr pour l'échantillon CEL 23 (Géosciences Rennes).

Sample	**Sm** (ppm)	**Nd** (ppm)	^{147}**Nd/**^{144}**Nd**	^{143}**Nd/**^{144}**Nd**	**error** $\times 10^{-6}$ ($\pm 2\sigma$ m)	ε_{Nd} (0 Ma)	ε_{Nd} (480 Ma)	T_{DM} (Ga)
CEL 23	10.27	52.93	0.1173	0.512 457	4	−3.6	1.3	1.10
CEL 23	10.13	51.92	0.1180	0.512 437	3	−4.0	0.9	1.13
Standard AMES	–	–	–	0.511 972	3			
	Rb (ppm)	**Sr** (ppm)	^{87}**Sr/**^{86}**Sr**	^{87}**Sr/**^{86}**Sr**	**error** $\times 10^{-6}$ ($\pm 2\sigma$ m)	I_{Sr} (480 Ma)		
CEL 23	110	34.3	9.33	0.766 221	6	0.7024		
Standard NBS 987	–	–	–	0.710 252	7			
Duplicate NBS 987	–	–	–	0.710 256	6			

Analytical procedures are described in [31].
Model ages have been calculated using the following depleted mantle values: $^{143}Nd/^{144}Nd = 0.513\,15$ ($\varepsilon_0 = +10$) and $^{147}Sm/^{144}Nd = 0.2137$.
ε_{Nd} values have been calculated with the following CHUR values: $^{143}Nd/^{144}Nd = 0.512\,64$ and $^{147}Sm/^{144}Nd = 0.1967$.
Errors on the Rb/Sr and Sm/Nd ratios are 2 and 0.2%, respectively.

of 1.1. The above characteristics are those of a high-K alkali feldspar granite, slightly alumina-saturated (A/CNK ca 1) and ferriferous ($Mg/(Mg + Fe) < 0.1$). Sample CEL 23 is thus a moderately fractionated alkaline granite. The low concentrations in Cs and Rb, the negative anomalies in Ba, Sr, Eu, P and Ti as well as the concave shape of the HREE (Fig. 3) indicate fractionation of feldspars, amphibole, apatite, titaniferous magnetite and probably biotite. The most remarkable geochemical characteristic of sample CEL 23 is the lack of significant anomalies for Ta, Nb and Pb (Th/Ta = 4.6, La/Nb = 1.31 and Ce/Pb = 13.3), which testify of the alkaline nature of the sample. The low value of the Ti/Nb ratio is consistent with this observation [2]. The Nb/Y, Ta/Yb, Rb/(Y + Nb), Rb/(Yb + Ta), Ga/Al values and the relations

Table 4. U/Pb analytical results for zircons from sample CEL 23 (BRGM, Orléans).
Tableau 4. Résultats analytiques U/Pb pour les zircons de l'orthogneiss du Cellier (sample CEL 23).

Fraction	Number of grains		Weight (µg)	Concentrations			Atomic ratios					Age
				U (ppm)	radio. Pb (ppm)	com. Pb (pg)	$^{206}Pb/^{204}Pb$	$^{208}Pb/^{206}Pb$	$^{206}Pb/^{238}U$	$^{207}Pb/^{235}U$	$^{207}Pb/^{206}Pb$	207/206
		[1]				[2]	[3]	[4]	[4]	[4]	[4]	(Ma)
1	3g	m5, op	67	1468	79.9	189	1792	0.0903	0.05519 ± 84	0.4307 ± 64	0.05660 ± 22	476
2	3g	m1, tr	26	597	35	48	1160	0.1235	0.05777 ± 20	0.4508 ± 18	0.05660 ± 10	476
3	3g	m1, tr	19	926	59.8	46	1534	0.115	0.06405 ± 72	0.5008 ± 56	0.05671 ± 16	480
4	4g	m1, tr	25	606	41.8	41	1528	0.1438	0.06673 ± 36	0.5219 ± 30	0.05672 ± 10	481
5	3g	m5, op	22	2859	152	104	2017	0.0998	0.05346 ± 40	0.4178 ± 32	0.05668 ± 8	479
6	3g	m5, op	26	1676	87.7	360	423	0.0655	0.05425 ± 28	0.4236 ± 26	0.05663 ± 16	477

1 = m1: magnetic for 1°; m5: magnetic for 5°; tr: translucent; op: opaque.
2 = total common lead (standard, blank and zircon).
3 = corrected for mass fractionation.
4 = corrected for mass fractionation, blank (Pb = 15 pg, U = 1 pg), standard and initial common Pb (calculated according to [35]). Errors of atomic ratios are given at 2σ level.

between Rb, Hf and Ta are typical of acid intraplate magmas [16, 29, 39]. More specifically, the low values of the Yb/Ta, Y/Nb and Ce/Nb ratios, as well as the Nb-rich composition in the ternary diagrams Nb/Y/(Ce or Ga), indicate that the protolith of sample CEL 23 was an A1-type granite (or rhyolite), i.e., was derived from a mantle source similar to those of the oceanic-island basalts (OIB) [10, 11]. The lack of major crustal contamination (because of the minor anomalies in Ta, Nb and Pb) implies a two-stage evolution, first fractionation of an underplated magma in a deep-seated chamber followed by high ascent velocity through dyking, preventing major crustal contamination.

The ε_{Nd} ratios at 480 Ma are ca +1 (Table 3), suggesting that the alkaline magma is derived from a depleted mantle (DM). Nevertheless, classical DM is more depleted at 480 Ma with ε_{Nd} ratios close to +9. This suggests that the T_{DM} model ages of 1.1 Ga measured are not significant, but indicate a mixing between a magma derived from a normal DM at 480 Ma, with an old crustal component (stricto sensu older than 1.1 Ga), probably ca 2 Ga old, as known in northern Brittany [14]. The ε_{Nd} values are in agreement with those reported for similar rocks in Galicia, NW Spain [33]. The initial Sr ratio at 480 Ma (0.702) is compatible with the mantle component previously defined, but could also result from an alteration of the Rb–Sr system during metamorphic processes.

5. Geochronology

Numerous zircons have been extracted from sample CL 23. They are generally subhedral; when euhedral, they are of the S22, P3 or P5 types [34], which are generally found in high temperature alkaline and calc-alkaline magmas. Analytical procedures are from Krogh [18] and Parrish [26], populations have been abraded following Krogh [19]. Analyses have been performed on a Finningan Mat 261 mass spectrometer using an electron multiplier system in dynamic mode. Pb and U blanks are lower than 15 and 1 pg, respectively. Final ratios are corrected from fractionation, blank, and initial common lead, using the two-stage model of Stacey and Kramers [35]. Errors are at two sigma (95% confidence level). The high U content (Table 4) explains probably the relative high degree of discordancy observed (14 to 30%) (Fig. 4). All the fractions have a restricted range of $^{207}Pb/^{206}Pb$ ages with a weighted average of 479 ± 2 Ma (using [23]). The discordia defines an upper intercept with an age of 481 $+6/-5$ Ma after the Davis regression programme [9]. The age of 481 ± 6 Ma is interpreted as the magmatic stage of this alkaline rock.

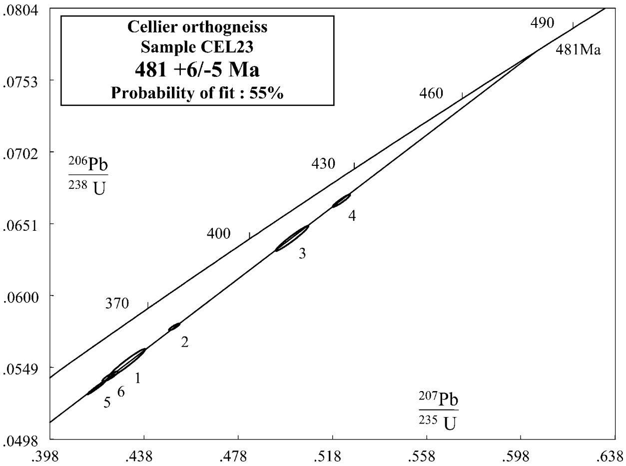

Figure 4. Concordia plot for the U–Pb analyses of zircons from the Cellier orthogneiss (sample CEL 23). Numbers refer to the fractions shown in Table 4.

Figure 4. Diagramme concordia U–Pb pour les zircons de l'orthogneiss du Cellier (échantillon CEL 23). Les chiffres correspondent aux fractions identifiées dans le Tableau 4.

6. Discussion and conclusion

The above data allow two main conclusions.

1. The biotite–hastingsite gneisses from the Cellier Unit (Champtoceaux Complex) derive from high-level intrusions (or volcanics) of typical alkaline affinity. The magmas crystallised during the Early Ordovician (at about 480 Ma). This Early Palaeozoic magmatism is largely represented in the Armorican Massif [17], either in units that have been slightly deformed during the Variscan Orogeny, like in the Choletais [22, 36] or as intensely strained rocks, like in the Champtoceaux Complex [28, and this study], the 'Golfe du Morbihan' [30], or the Concarneau area [4, 15, 37]. Alkaline protoliths are now identified in the Concarneau area [37], the Choletais area [36] and the Champtoceaux Complex (this study).

2. As usual, orthogneisses are poor recorders of the metamorphic evolution. Mineral parageneses within the biotite–hastingsite gneisses indicate nearly complete reequilibration at epidote–amphibolite facies conditions. Potential relics of the eclogite-facies event in the alkaline orthogneisses are coexisting grossular-rich garnet and rutile (cf. [6]).

3. Alkaline orthogneisses are known in several eclogite-bearing units from the Variscan Belt (e.g. [12, 33, this study]). Accordingly, continental subduction in the Variscan Belt mainly took place at the expense of a continental crust, which was significantly thinned through intracontinental rifting of Cambro-Ordovician age. This represents a major contrast with the Alpine Belt, where continental subduction involves burial of the passive palaeomargins, where syn-rifiting magmatism is either poorly developed or lacking.

References

[1] M. Ballèvre, J. Marchand, Zonation du métamorphisme éclogitique dans la nappe de Champtoceaux (Massif armoricain, France), C. R. Acad. Sci. Paris, série D 312 (1991) 705–711.

[2] J.-L. Bonjour, M.-P. Dabard, Ti/Nb ratios of clastic terrigenous sediments used as an indicator of provenance, Chem. Geol. 91 (1991) 257–267.

[3] V. Bosse, G. Féraud, G. Ruffet, M. Ballèvre, J.-J. Peucat, K. de Jong, Late Devonian subduction and early-orogenic exhumation of eclogite-facies rocks from the Champtoceaux Complex (Variscan Belt, France), Geol. J. 35 (2000) 337–350.

[4] J.-Y. Calvez, Comportements des sytèmes uranium–plomb et rubidium–strontium dans les orthogneiss d'Icart et de Moëlan (Massif armoricain), thèse 3ème cycle, université de Rennes, 1976, 74 p.

[5] F. Chen, E. Hegner, W. Todt, Zircon ages and Nd isotopic and chemical compositions of orthogneisses from the Black Forest, Germany: evidence for a Cambrian magmatic arc, Int. J. Earth Sci. 88 (2000) 791–802.

[6] C. Chopin, C. Henry, A. Michard, Geology and petrology of the coesite-bearing terrain, Dora-Maira massif, Western Alps, Eur. J. Mineral. 3 (1991) 263–291.

[7] J. Cogné, Une nappe cadomienne de style pennique : la série cristallophyllienne de Champtoceaux en bordure méridionale du synclinal d'Ancenis (Bretagne–Anjou), Bull. Serv. Carte Géol. Als.-Lorr. 19 (1966) 107–136.

[8] Q.G. Crowley, P.A. Floyd, J.A. Winchester, W. Franke, J.-G. Holland, Early Palaeozoic rift-related magmatism in Variscan Europe: fragmentation of the Armorican Terrane Assemblage, Terra Nova 12 (2000) 171–180.

[9] D.W. Davis, Optimum linear regression and error estimation applied to U–Pb data, Can. J. Earth Sci. 19 (1982) 2141–2149.

[10] G.N. Eby, The A-type granitoids: a review of their occurrence and chemical characteristics and speculations on their petrogenesis, Lithos 26 (1990) 115–134.

[11] G.N. Eby, Chemical subdivision of the A-type granitoids: petrogenetic and tectonic implications, Geology 20 (1992) 641–644.

[12] P. Floor, Petrology of an aegirine-riebeckite gneiss-bearing part of the Hesperian Massif: The Galineiro and surrounding areas, Vigo, Spain, Leidse Geol. Meded. 36 (1966) 1–203.

[13] G. Godard, Petrology of some eclogites from in the Hercynides: the eclogites from the southern armorican massif, France, in: D.C. Smith (Ed.), Eclogites and eclogite-facies rocks, Elsevier, Amsterdam, 1988, pp. 451–519.

[14] C. Guerrot, Archéen et Protérozoique dans la chaîne hercynienne ouest européenne, Mém. Doc. Centre Arm. Et. St. Socles 25, 1989, 164 p.

[15] C. Guerrot, F. Béchennec, D. Thiéblemont, Le magmatisme paléozoïque de la partie nord-ouest du domaine sud-armoricain : données géochronologiques nouvelles, C. R. Acad. Sci. Paris, série IIa 324 (1997) 977–984.

[16] N.B.W. Harris, J.A. Pearce, A.G. Tindle, The geochemical characteristics of collision-zone magmatism, Geol. Soc. London Spec. Publ. 19 (1986) 67–81.

[17] P. Jegouzo, J.-J. Peucat, C. Audren, Caractérisation et signification géodynamique des orthogneiss calco-alcalins d'âge Ordovicien de Bretagne méridionale, Bull. Soc. géol. France II (8) (1986) 839–848.

[18] T.E. Krogh, A low-contamination method for hydrothermal decomposition of zircon and extraction of U and Pb for isotopic age determination, Geochim. Cosmochim. Acta 37 (1973) 485–494.

[19] T.E. Krogh, Improved accuracy of U–Pb zircon ages by the creation of more concordant systems using an air abrasion technique, Geochim. Cosmochim. Acta 46 (1982) 637–649.

[20] B. Lasnier, A. Leyreloup, J. Marchand, Découverte d'un granite « charnockitique » au sein des « gneiss œillés ». Perspectives nouvelles sur l'origine de certaines leptynites du Massif armoricain méridional (France), Contrib. Mineral. Petrol. 41 (1973) 131–144.

[21] É. Le Goff, M. Ballèvre, Méthodes d'estimation des conditions P–T dans les orthogneiss : analyse des relations de phases, C. R. Acad. Sci. Paris, série II 311 (1990) 119–125.

[22] J. Le Métour, J. Bernard-Griffiths, Âge (limite Ordovicien–Silurien) de mise en place du massif hypovolcanique de Thouars (Massif vendéen). Implications géologiques, Bull. BRGM 4 (1979) 365–371.

[23] R.K. Ludwig, Isoplot 2.06. A geochronological toolkit for Microsoft Excel, Special Publ. 1a, Berkeley Geochronology Center, 1999, 49 p.

[24] J. Marchand, Écaillage d'un « mélange tectonique » profond : le complexe cristallophyllien de Champtoceaux (Bretagne méridionale), C. R. Acad. Sci. Paris, série II 293 (1981) 223–228.

[25] J. Marchand, D. Sellier, G. Bossière, avec la collaboration de G. Carlier, C. Deniel, B. Lasnier, Carte géologique de France (1:50 000), feuille Savenay (450), Bur. Rech. Géol. Min., Orléans, 1989.

[26] R.R. Parrish, An improved micro-capsule for zircon dissolution in U–Pb geochronology, Chem. Geol. 66 (1987) 99–102.

[27] J.-L. Paquette, Comportement des systèmes isotopiques U–Pb et Sm–Nd dans le métamorphisme éclogitique. Chaîne hercynienne et chaîne alpine, Mém. Doc. Centre Arm. Ét. St. Socles 14 (1987) 1–190.

[28] J.-L. Paquette, J. Marchand, J.-J. Peucat, Absence de tectonique cadomienne dans le complexe de Champtoceaux (Bretagne méridionale) ? Comparaison des systèmes Rb–Sr et U–Pb d'un métagranite, Bull. Soc. géol. France XXVI (7) (1984) 907–912.

[29] J.A. Pearce, N.B.W. Harris, A.G. Tindle, Trace element discrimination diagrams for the tectonic interpretation of granitic rocks, J. Petrol. 25 (1984) 956–983.

[30] J.-J. Peucat, J. Le Métour, C. Audren, Arguments géochronologiques en faveur de l'existence d'une double ceinture métamorphique d'âge Siluro-Dévonien en Bretagne méridionale, Bull. Soc. géol. France XX (7) (1978) 163–167.

[31] J.-J. Peucat, R.-P. Ménot, O. Monnier, C.M. Fanning, The Terre Adélie basement in the East-Antarctica shield: geological and isotopic evidence for a major 1.7 Ga thermal event; comparison with the Gawler Craton in South Australia, Precambr. Res. 94 (1999) 205–224.

[32] C. Pin, F. Marini, Early Ordovician continental break-up in Variscan Europe: Nd–Sr isotope and trace element evidence from bimodal igneous associations of the southern Massif Central, France, Lithos 29 (1993) 177–186.

[33] C. Pin, L.A. Ortega Cuesta, I. Gil Ibarguchi, Mantle-derived, Early-Palaeozoic A-type meta-granitoids from the NW Iberian Massif: Nd isotope and trace-elements constraints, Bull. Soc. géol. France 163 (1992) 483–494.

[34] J.-P. Pupin, Zircon and granite petrology, Contrib. Mineral. Petrol. 73 (1980) 207–220.

[35] J.S. Stacey, J.D. Kramers, Approximation of terrestrial lead isotope evolution by a two-stage model, Earth Planet. Sci. Lett. 26 (1975) 207–221.

[36] D. Thiéblemont, B. Cabanis, J. Le Métour, Étude géochimique d'un magmatisme de distension intracontinentale : la série bimodale ordovicienne du Choletais (Massif vendéen), Géol. France 1 (1987) 65–76.

[37] D. Thiéblemont, F. Béchennec, B. Cabanis, J. Chantraine, Lithostratigraphie et géochimie des formations paléomagmatiques dans le secteur Moëlan–Concarneau (Bretagne méridionale). Nouvelles contraintes sur l'évolution géodynamique du domaine sud-armoricain au cours du Paléozoïque, Geodin. Acta 3 (2) (1989) 1–16.

[38] P. Vidal, J.-J. Peucat, B. Lasnier, Dating of granulites involved in the Hercynian fold belt of Europe: an example taken from the granulite-facies orthogneiss at la Picherais, Southern Armorican Massif, France, Contrib. Mineral. Petrol. 72 (1980) 283–289.

[39] J.B. Whalen, K.L. Currie, B.W. Chappell, A-type granites: chemical characteristics, discrimination and petrogenesis, Contrib. Mineral. Petrol. 95 (1987) 407–419.